J|A|C|S ARTICLES

Published on Web 08/28/2009

Directly Relating Reduction Energies of Gaseous $Eu(H_2O)_n^{3+}$, $n = 55-140$, to Aqueous Solution: The Absolute SHE Potential and Real Proton Solvation Energy

William A. Donald, Ryan D. Leib, Maria Demireva, Jeremy T. O'Brien, James S. Prell, and Evan R. Williams*

Department of Chemistry, University of California, Berkeley, California 94720-1460

Received April 8, 2009; E-mail: williams@cchem.berkeley.edu

Abstract: In solution, half-cell potentials are measured relative to other half-cells resulting in a ladder of thermodynamic values that is anchored to the standard hydrogen electrode (SHE), which is assigned an arbitrary value of exactly 0 V. A new method for measuring the absolute SHE potential is introduced in which reduction energies of $Eu(H_2O)_n^{3+}$, from $n = 55$ to 140, are extrapolated as a function of the geometric dependence of the cluster reduction energy to infinite size. These measurements make it possible to directly relate absolute reduction energies of these gaseous nanodrops containing Eu^{3+} to the absolute reduction enthalpy of this ion in bulk solution. From this value, an absolute SHE potential of +4.11 V and a real proton solvation energy of −269.0 kcal/mol are obtained. The infrared photodissociation spectrum of $Eu(H_2O)_{119-124}^{3+}$ indicates that the structure of the surface of the nanodrops is similar to that at the bulk air−water interface and that the hydrogen bonding of interior water molecules is similar to that in aqueous solution. These results suggest that the environment of Eu^{3+} in these nanodrops and the surface potential of the nandrops are comparable to those of the condensed phase. This method for obtaining absolute potentials of redox couples has the advantage that no explicit solvation model is required, which eliminates uncertainties associated with these models, making this method potentially more accurate than previous methods.

Introduction

In solution, reduction potentials of half-cells are not measured in isolation, but rather are measured relative to the potentials of other half-cells, resulting in a ladder of relative thermochemical redox potentials. This relative ladder of values is anchored to the standard hydrogen electrode (SHE), $H^+ + e^- \rightarrow {}^1/_2H_2(g)$, which is arbitrarily assigned a redox potential of exactly 0 V. If an absolute potential of a single half-cell could be accurately measured, an absolute electrochemical scale could be established. Determining absolute electrode potentials has been a subject of considerable interest, which has led to the development of many different approaches to solving this problem.[1−14] However, because previous experimental approaches to obtain absolute potentials have been indirect, and because of the relatively wide range of reported values from different methods, this topic remains controversial.[1−14] These factors have led Trasatti to conclude about the absolute electrode potential that "despite the numerous discussions, nobody seems seriously convinced of the arguments of the others."[1]

A widely accepted definition of the absolute SHE potential is the reduction potential of an aqueous proton referenced to a gaseous electron at infinite distance.[2] The absolute Gibbs free energy of the SHE reaction, $\Delta G_{abs}(SHE)$ (which is related to the standard redox potential, $E°$, by $\Delta G = -nFE°$, where n is the number of transferred electrons and F is the Faraday constant), is given by

$$\Delta G_{abs}(SHE) = -\Delta G_{at}(\tfrac{1}{2}H_2) - \Delta G_{ion}(H) - \alpha(H^+,aq) \quad (1)$$

where $\Delta G_{at}({}^1/_2H_2)$ and $\Delta G_{ion}(H)$ are the atomization and ionization energies of molecular and atomic hydrogen, respectively, and $\alpha(H^+,aq)$ is the real proton solvation free energy. This latter value can be expressed as

$$\alpha(H^+,aq) = \mu(H^+,aq) + e\chi(aq) \quad (2)$$

where $\mu(H^+,aq)$ is the chemical potential of the hydrated proton, e is the elementary charge, and $\chi(aq)$ is the surface potential of the bulk air−water interface as a result of the orientation of

(1) Trasatti, S. *Electrochim. Acta* **1990**, *35*, 269–271.
(2) Trasatti, S. *Pure Appl. Chem.* **1986**, *58*, 955–966.
(3) Parsons, R. In *Standard Potentials in Aqueous Solution*; Bard, A. J., Parsons, R., Jordan, J., Eds.; Marcel Dekker: New York, 1985; pp 13−37.
(4) Gomer, R.; Tryson, G. *J. Chem. Phys.* **1977**, *66*, 4413–4424.
(5) Hansen, W. N.; Kolb, D. M. *J. Electroanal. Chem.* **1979**, *100*, 493–500.
(6) Kelly, C. P.; Cramer, C. J.; Truhlar, D. G. *J. Phys. Chem. B* **2006**, *110*, 16066–16081.
(7) Kelly, C. P.; Cramer, C. J.; Truhlar, D. G. *J. Phys. Chem. B* **2007**, *111*, 408–422.
(8) Fawcett, W. R. *Langmuir* **2008**, *24*, 9868–9875.
(9) Hansen, W. N.; Hansen, G. J. *Phys. Rev. A* **1987**, *36*, 1396–1402.
(10) Reiss, H. *J. Electrochem. Soc.* **1988**, *135*, 247C–258C.
(11) Reiss, H.; Heller, A. *J. Phys. Chem.* **1985**, *89*, 4207–4213.
(12) Trasatti, S. *Electrochim. Acta* **1991**, *36*, 1659–1667.
(13) Trasatti, S. *J. Electroanal. Chem.* **1982**, *139*, 1–13.
(14) Gerischer, H.; Ekardt, W. *Appl. Phys. Lett.* **1983**, *43*, 393–395.

10.1021/ja902815v CCC: $40.75

water molecules at the interface. Trasatti has recommended a value of +4.44 V for the absolute SHE potential[2] to the International Union of Pure and Applied Chemists that is obtained from a value of −260.0 kcal/mol for $\alpha(H^+,aq)$ that was reported by Farrell and McTigue.[15] This latter value is obtained from the extrapolation of experimental measurements of the potential across a high resistance electrochemical cell from 1 mM HCl concentration to infinite dilution using a theoretical model[16] of the dependence of the surface potential of the air−aqueous HCl interface on electrolyte concentration. The surface potential of the HCl solution is assumed to vary monotonically and linearly from 20 mM to infinite dilution. Because this method uses a theoretical model for the surface potential dependence on ion concentration[16] and because of the controversy[17−19] as to what the surface potential of water is and the wide range of values that have been reported for this potential (−1.1 to +0.5 V),[17−19] it is interesting to compare the $\chi(aq)$ value reported by Farrell and McTigue (+25 mV) to that obtained from more recent calculations. For example, a value of −18 mV for the surface potential of pure water[18] was recently reported from quantum chemical calculations. If the surface potential of water is negative or much different from +25 mV, then the values obtained for $\alpha(H^+,aq)$ and the absolute SHE potential from this method could be different as well.

Other methods have been used to obtain a value for the absolute SHE potential. From the experimentally measured potential differences between immersed and emersed electrodes, values of +4.7[5] and +4.73 V[4] have been reported. However, reorientation of adsorbed solvent molecules at the surface of electrodes upon emersion versus immersion may explain the difference between the value from these experiments and other lower estimates for the absolute SHE potential.[20] Another method to obtain the absolute SHE potential is to determine $\mu(H^+,aq)$ and combine this value with the surface potential of water, using eqs 1 and 2. Various computational methods have been used to obtain values for the solvation free energy of the proton that range from −254.4 to −266.7 kcal/mol.[21−23] A cluster-pair correlation scheme, which uses extensive gas-phase clustering experimental data, has also been used to obtain a value of −265.9 kcal/mol (reported using the reference state given in ref 6) for the solvation free energy of the proton.[6,7,24−26] Relating these reported values for the solvation free energy of the proton to the SHE potential may be complicated because of apparent controversy as to whether or not some of these values include $\chi(aq)$.[7,8,21,22] Using the most recent value of $\chi(aq)$, −18 mV, from quantum-mechanical molecular dynamics calculations, absolute SHE potential values between +4.2 and +4.7 V are obtained from the range of reported values for the proton solvation free energy.

An alternative route to investigating condensed-phase physical properties is from gas-phase studies of clusters[27−30] or isolated molecules.[31−36] For example, properties of the hydrated electron have been inferred from gas-phase studies of water clusters with an excess electron.[37−43] "Aqueous" nanodrops have also been shown to demonstrate other interesting bulk-like properties. For example, $M^+(H_2O)_n$, M = Cr, Mn, Fe, Co, Ni, Cu, Na, and Ag, clusters can dissolve HCl(g) molecules and "precipitate" M(I)Cl in the form of $H^+(H_2O)_n(MCl)$ at large enough cluster sizes.[44,45] Other clusters containing Mg, Al, or V result in metal ion oxidation by the dissolved HCl.[44,46,47] The change in reactivity correlates with the oxidation potentials of the metals.[44] Other studies have shown correlations between the first ionization energies[31−34,36] (or electron affinities)[33,35] in the gas phase and the one-electron reduction potentials in nonaqueous solution for a series of neutral aromatic compounds. The degree of correlation between the gas- and solution-phase data depends strongly upon solvent effects,[31] which has limited such studies to investigations of molecules and solvents in which these effects remain relatively constant or negligible. These results highlight the complications in directly comparing absolute gas-phase ionization energies to the corresponding absolute reduction potentials in the condensed phase.

Because of the wide range of reported values from previous indirect experimental measurements and computational approaches, it is interesting to develop more direct measurements of reduction potentials. We recently introduced a gaseous ion nanocalorimetry technique,[48−56] in which gas-phase electrochemistry is performed using large aqueous nanodrops to obtain

(15) Farrell, J. R.; McTigue, P. *J. Electroanal. Chem.* **1982**, *139*, 37–56.
(16) Madden, W. G.; Gomer, R.; Mandell, M. J. *J. Phys. Chem.* **1977**, *81*, 2652–2657.
(17) Sokhan, V. P.; Tildesley, D. J. *Mol. Phys.* **1997**, *92*, 625–640.
(18) Kathmann, S. M.; Kuo, I.-F. W.; Mundy, C. J. *J. Am. Chem. Soc.* **2008**, *130*, 16556–16561.
(19) Randles, J. E. B. *Phys. Chem. Liq.* **1977**, *7*, 107–179.
(20) Samec, Z.; Johnson, B. W.; Doblhofer, K. *Surf. Sci.* **1992**, *264*, 440–448.
(21) Bryantsev, V. S.; Diallo, M. S.; Goddard, W. A., III. *J. Phys. Chem. B* **2008**, *112*, 9709–9719.
(22) Asthagiri, D.; Pratt, L. R.; Ashbaugh, H. S. *J. Chem. Phys.* **2003**, *119*, 2702–2707.
(23) Zhan, C.-G.; Dixon, D. A. *J. Phys. Chem. A* **2001**, *2001*, 11534–11540.
(24) Tissandier, M. D.; Cowen, K. A.; Feng, W. Y.; Gundlach, E.; Cohen, M. H.; Earhart, A. D.; Coe, J. V.; Tuttle, T. R., Jr. *J. Phys. Chem. A* **1998**, *102*, 7787–7794.
(25) Tuttle, T. R., Jr.; Malaxos, S.; Coe, J. V. *J. Phys. Chem. A* **2002**, *106*, 925–932.
(26) Coe, J. V. *Int. Rev. Phys. Chem.* **2001**, *20*, 33–58.
(27) Castleman, A. W., Jr.; Bowen, K. H., Jr. *J. Phys. Chem.* **1996**, *100*, 12911–12944.
(28) Beyer, M. *Mass Spectrom. Rev.* **2007**, *26*, 517–541.
(29) Meot-Ner, M. *Chem. Rev.* **2005**, *105*, 213–284.
(30) Kebarle, P. *Annu. Rev. Phys. Chem.* **1977**, *28*, 445–476.
(31) Pysh, E. S.; Yang, N. C. *J. Am. Chem. Soc.* **1963**, *85*, 2124–2130.
(32) Howell, J. O.; Goncalves, J. M.; Amatore, C.; Klasinc, L.; Wightman, R. M.; Kochi, J. K. *J. Am. Chem. Soc.* **1984**, *106*, 3968–3976.
(33) Parker, V. D. *J. Am. Chem. Soc.* **1976**, *98*, 98–103.
(34) Masnovi, J. M.; Seddon, E. A.; Kochi, J. K. *Can. J. Chem.* **1984**, *62*, 2552–2559.
(35) Peover, M. E. *Nature* **1962**, *193*, 475–476.
(36) Wentworth, W. E.; Chen, E. *J. Phys. Chem.* **1967**, *71*, 1929–1931.
(37) Coe, J. V.; Lee, G. H.; Eaton, J. G.; Arnold, S. T.; Sarkas, H. W.; Bowen, K. H.; Ludewigt, C.; Haberland, H.; Worsnop, D. R. *J. Chem. Phys.* **1990**, *92*, 3980–3982.
(38) Coe, J. V.; Williams, S. M.; Bowen, K. H. *Int. Rev. Phys. Chem.* **2008**, *27*, 27–51.
(39) Verlet, J. R. R.; Bragg, A. E.; Kammrath, A.; Cheshnovsky, O.; Neumark, D. M. *Science* **2005**, *307*, 93–96.
(40) Paik, D. H.; Lee, I.-R.; Yang, D.-S.; Baskin, J. S.; Zewail, A. H. *Science* **2004**, *306*, 672–675.
(41) Bragg, A. E.; Verlet, J. R. R.; Kammrath, A.; Cheshnovsky, O.; Neumark, D. M. *Science* **2004**, *306*, 669–671.
(42) Hammer, N. I.; Shin, J.-W.; Headrick, J. M.; Diken, E. G.; Roscioli, J. R.; Weddle, G. H.; Johnson, M. A. *Science* **2004**, *306*, 675–679.
(43) Asmis, K. R.; Santambrogio, G.; Zhou, J.; Garand, E.; Headrick, J.; Goebbert, D.; Johnson, M. A.; Neumark, D. M. *J. Chem. Phys.* **2007**, *126*, 191105.
(44) Fox, B. S.; Balaj, O. P.; Balteanu, I.; Beyer, M. K.; Bondybey, V. E. *J. Am. Chem. Soc.* **2002**, *124*, 172–173.
(45) Fox-Beyer, B. S.; Sun, Z.; Balteanu, I.; Balaj, O. P.; Beyer, M. K. *Phys. Chem. Chem. Phys.* **2005**, *7*, 981–985.
(46) Berg, C.; Beyer, M.; Achatz, U.; Joos, S.; Niedner-Schatteburg, G.; Bondybey, V. E. *Chem. Phys.* **1998**, *239*, 379–392.
(47) Beyer, M.; Achatz, U.; Berg, C.; Joos, S.; Niedner-Schatteburg, G.; Bondybey, V. E. *J. Phys. Chem. A* **1999**, *103*, 671–678.
(48) Donald, W. A.; Leib, R. D.; O'Brien, J. T.; Bush, M. F.; Williams, E. R. *J. Am. Chem. Soc.* **2008**, *130*, 3371–3381.

absolute half-cell potentials in the condensed phase.[48,49] Water clusters containing Cu^{2+} and $M(NH_3)_6^{3+}$, for M = Ru, Co, Os, Cr, and Ir, that capture thermally generated electrons result in the loss of water molecules from the reduced droplet.[48] The adiabatic ion-electron recombination energy (RE) is equal to the energy removed by the lost water molecules. Solvent reorganization energy resulting from the change in ion charge state is reflected in the measured RE. The REs can be related to absolute reduction potentials in bulk solution using a solvation model, which results in values that strongly correlate with the relative solution-phase reduction potentials. From the absolute reduction potentials and the experimental relative potentials in solution,[48] a value for the absolute SHE of +4.2 V was obtained. Very recently,[50] we introduced a second, largely independent method to obtain the absolute SHE potential. From the RE values for reduction of hydrated $M(H_2O)_{24}^{2+}$, M = Mg, Ca, Sr, Mn, Fe, Co, Ni, Cu, and Zn, that results in the loss of an H atom and water molecules, and a thermodynamic cycle that includes solution hydrolysis, a value for the absolute SHE potential of +4.29 V (revised here to +4.05 V; see Supporting Information) was obtained. This method has the advantage that ions that do not undergo one-electron reduction in solution may be used to obtain the absolute SHE potential; that is, solution-phase redox potentials are not used.

Here, the reduction energies of size-selected $Eu(H_2O)_n^{3+}$ with n from 55 to 140 are measured using ion nanocalorimetry. These values are extrapolated to infinite cluster size to obtain an absolute reduction enthalpy for Eu^{3+} in aqueous solution. In combination with an experimental value for reduction entropy, the absolute free energy of reduction and hence the absolute reduction potential are obtained. From this value, the absolute SHE potential and real proton solvation energy are determined. This method is largely independent of our other two nanocalorimetry methods used to obtain an absolute SHE potential, and this method has the advantage that no solvation models are used, eliminating sources of error associated with these models. This is the most direct measurement of an absolute reduction potential and could potentially be the most accurate way to establish an absolute electrochemical redox scale.

Experimental Section

Nanocalorimetry experiments are performed on a 2.75 T Fourier transform ion cyclotron resonance (FT/ICR) mass spectrometer equipped with a cooled ion cell that is equilibrated to a temperature of −140 °C;[51,53,57,58] select experiments are performed with the ion cell equilibrated to either −110 or −90 °C. Ions are generated by nanoelectrospray of 1−5 mM aqueous solutions of $EuCl_3$. A potential of +500 to +800 V relative to the heated (~80 °C) entrance capillary of the mass spectrometer is applied to a Pt wire that is in direct contact with the $EuCl_3$ solution contained in a borosilicate capillary that has an inner tip diameter of ~1 μm. Ions are guided into the ion cell through five stages of differential pumping, accumulated for 3−9 s, during which time dry N_2(g) is pulsed into the vacuum chamber to a pressure of $\sim 10^{-6}$ Torr using a piezoelectric valve to enhance the trapping and thermalization of the ions. Ions are then stored for an additional 4−10 s to allow the vacuum chamber pressure to return to $\leq 10^{-8}$ Torr and to ensure the ions have steady state internal energy distributions at the temperature of the copper jacket (−140 °C) surrounding the ion cell.

For electron capture (EC) experiments,[51,53] ions are isolated using SWIFT waveforms. Following a 40 ms delay, electrons are introduced into the ion cell from a heated dispenser cathode (Heatwave Laboratories, Watsonville, CA) mounted axially 20 cm from the cell center that is pulsed to a potential of −1.5 V for 120 ms. A delay of 1.00 s between the end of electron introduction and before ion excitation/detection is used to ensure that the dissociation of the reduced cluster is complete. A potential of +10 V is applied to the cathode at all other times to prevent electrons from entering the cell. A Cu wire mesh mounted 0.5 cm in front of the cathode is held at a potential of +9 V.

The average number of water molecules lost from the reduced precursor is obtained from a weighted average of the observed product ion distribution and is corrected for the blackbody infrared radiative absorption loss of water molecules that occurs in the absence of EC to give the average number of water molecules lost due to EC alone. Internal energies were calculated as described previously[48] using calculated harmonic frequencies for an energy-minimized B3LYP/LACVP**++ structure for $Ca(H_2O)_{14}^{2+}$. Internal energies were obtained by linearly scaling the degrees-of-freedom of $Ca(H_2O)_{14}^{2+}$ by the degrees-of-freedom of the cluster of interest.

To obtain a photodissociation spectrum of $Eu(H_2O)_n^{3+}$, a distribution of ions from n = 119 to 124 is isolated using SWIFT waveforms and irradiated with tunable infrared light in the OH stretch region (~3000−3800 cm^{-1}) from an OPO/OPA laser system that has been described in detail elsewhere.[59] An irradiation time of 2 s (20 laser pulses) is used to achieve significant photodissociation for free and bonded OH stretch features. The relative intensities are obtained from the average number of water molecules lost from the initial $Eu(H_2O)_n^{3+}$ distribution upon laser irradiation as a function of photon energy. These values are corrected for dissociation resulting from the absorption of blackbody infrared photons from the 133 K ion cell and cell jacket and variations in the laser power with frequency.

Results and Discussion

Electron Capture by Size-Selected $Eu(H_2O)_n^{3+}$. Nanoelectrospray of aqueous solutions containing $EuCl_3$ results in the formation of broad distributions of $Eu(H_2O)_n^{3+}$ and $EuOH(H_2O)_n^{2+}$ clusters, which can be shifted to larger (Figure 1a) or to smaller cluster sizes (Figure 1b), by changing instrumental parameters.[57] Experimental conditions for the mass spectrum shown in Figure 1b were optimized for $Eu(H_2O)_{55}^{3+}$; results of isolating and subsequently reacting this ion with thermally generated electrons for 120 ms are shown in Figure 1c. Electron capture (EC) by $Eu(H_2O)_{55}^{3+}$ results in the loss of 16−19 water molecules from the reduced cluster (Figure 1c). Water molecule loss from the precursor ion also occurs (34%) as a result of absorption of blackbody infrared radiation from the cooled ion cell and surrounding copper jacket as well as

(49) Leib, R. D.; Donald, W. A.; O'Brien, J. T.; Bush, M. F.; Williams, E. R. *J. Am. Chem. Soc.* **2007**, *129*, 7716–7717.
(50) Donald, W. A.; Leib, R. D.; O'Brien, J. T.; Williams, E. R. *Chem.-Eur. J.* **2009**, *15*, 5926–5934.
(51) Leib, R. D.; Donald, W. A.; Bush, M. F.; O'Brien, J. T.; Williams, E. R. *J. Am. Soc. Mass Spectrom.* **2007**, *18*, 1217–1231.
(52) Leib, R. D.; Donald, W. A.; Bush, M. F.; O'Brien, J. T.; Williams, E. R. *J. Am. Chem. Soc.* **2007**, *129*, 4894–4895.
(53) O'Brien, J. T.; Prell, J. S.; Holm, A. I. S.; Williams, E. R. *J. Am. Soc. Mass Spectrom.* **2008**, *19*, 772–779.
(54) Donald, W. A.; Leib, R. D.; O'Brien, J. T.; Holm, A. I. S.; Williams, E. R. *Proc. Natl. Acad. Sci. U.S.A.* **2008**, *105*, 18102–18107.
(55) Prell, J. S.; O'Brien, J. T.; Holm, A. I. S.; Leib, R. D.; Donald, W. A.; Williams, E. R. *J. Am. Chem. Soc.* **2008**, *130*, 12680–12689.
(56) Holm, A. I. S.; Donald, W. A.; Hvelplund, P.; Larsen, M. K.; Nielsen, S. B.; Williams, E. R. *J. Phys. Chem. A* **2008**, *112*, 10721–10727.
(57) Bush, M. F.; Saykally, R. J.; Williams, E. R. *Int. J. Mass Spectrom.* **2006**, *253*, 256–262.
(58) Wong, R. L.; Paech, K.; Williams, E. R. *Int. J. Mass Spectrom.* **2004**, *232*, 59–66.
(59) Bush, M. F.; O'Brien, J. T.; Prell, J. S.; Saykally, R. J.; Williams, E. R. *J. Am. Chem. Soc.* **2007**, *129*, 1612–1622.

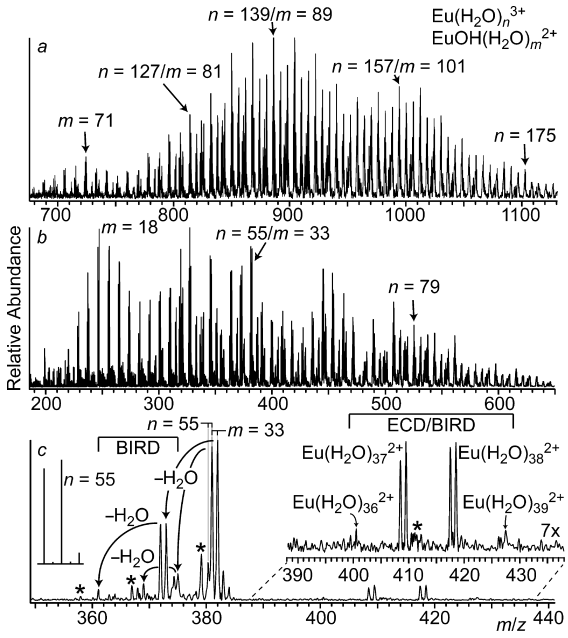

Figure 1. Nanoelectrospray mass spectra of $Eu(H_2O)_n^{3+}$ and $EuOH(H_2O)_m^{2+}$ optimized for (a) larger and (b) smaller cluster sizes, and (c) electron capture mass spectrum of $Eu(H_2O)_{55}^{3+}$ resulting in the loss of 16−19 water molecules from the reduced precursor as a result of electron capture dissociation (ECD) and blackbody infrared radiative dissociation (BIRD). Up to two water molecules are lost from $Eu(H_2O)_{55}^{3+}$ and $EuOH(H_2O)_{33}^{2+}$ as a result of BIRD. The theoretical isotope distribution of $Eu(H_2O)_{55}^{3+}$ is inset (left) in (c). The peak at $m/z = 381$ contains a ~24% contribution from $Eu(H_2O)_{55}^{3+}$ and ~76% contribution from $EuOH(H_2O)_{33}^{2+}$. Asterisks mark peaks corresponding to $H(H_2O)_{21}^{+}$ (m/z = 379), $H(H_2O)_{20}^{+}$ (m/z = 361), $Eu(OH)_2(H_2O)^{+}$ (m/z = 367), and instrumental noise (m/z = 411).

from the heated cathode located 20 cm from the cell. Previous experiments with $Ca(H_2O)_n^{2+}$ indicate that inelastic collisions with electrons and collisions with residual gas in the ion cell do not affect the extent of water molecule loss from the precursor or the reduced precursor under these conditions, nor does the initial electron kinetic energy because EC is most efficient when the relative kinetic energy between the ion and electron approaches zero.[53] The average number of water molecules lost due to EC of $Eu(H_2O)_{55}^{3+}$ alone can be obtained by correcting the observed average number of water molecules lost from the reduced precursor (17.5 water molecules) for the average number of water molecules lost due to blackbody infrared radiative dissociation (BIRD), which is estimated from the average number of water molecules lost from the precursor ion (0.4 water molecules). That is, the average number of water molecules lost due to EC alone is 17.5 − 0.4 = 17.1. Although the number of water molecules lost is large, the product ion distribution is remarkably narrow (Figure 1c).

The average number of water molecules lost resulting from EC by size-selected $Eu(H_2O)_n^{3+}$ was obtained for n between 50 and 140 (Figure 2). For $n \geq 55$, the average number of water molecules lost decreases with increasing cluster sizes. This effect is primarily attributed to increasing ion solvation with increasing cluster size,[48,54] which results in a lower RE. Under these conditions, collisional and radiative cooling are expected to be minimal. By comparison, the average number of water molecules lost upon EC by $Ru(NH_3)_6(H_2O)_n^{3+}$ for $n \leq 40$[49] decreases with decreasing cluster size as a result of increasing water binding energies and increasing energy partitioning into translational and rotational modes of the products. For n between

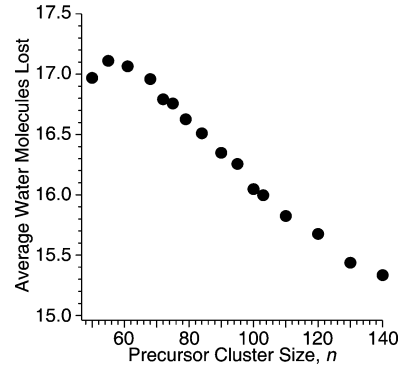

Figure 2. The average number of water molecules lost from reduced $Eu(H_2O)_n^{3+}$ as a result of electron capture as a function of the precursor cluster size, n.

40 and 55, a broad plateau in the average number of water molecules lost occurs and reflects competing effects of ion solvation versus water binding energy and energy partitioning effects.[49] Fewer water molecules are lost upon EC of $Ru(NH_3)_6(H_2O)_{61}^{3+}$ than $Ru(NH_3)_6(H_2O)_{55}^{3+}$,[49] consistent with the results for $Eu(H_2O)_n^{3+}$ reported here.

Dissociation Time Scale. For small clusters, dissociation upon EC is fast as compared to the time scale of the experiment.[51] For clusters with $n \geq 55$, the RE decreases with increasing cluster size due to improved ion solvation, whereas the number of degrees-of-freedom in a cluster increases with size. Thus, the effective temperature to which a cluster is heated decreases with increasing cluster size. This results in a slower rate of water evaporation from the cluster upon EC with increasing cluster size. To obtain accurate RE values from these nanocalorimetry experiments, water evaporation after EC must be complete prior to product ion detection; that is, the reduced cluster must return to close to the initial temperature at the start of the experiment. In addition, competitive processes, such as collisional energy transfer to background gas or radiative cooling, must be slow as compared to the rate of water molecule loss.

To investigate the rate at which water evaporation occurs for the larger clusters in this study, $Eu(H_2O)_n^{3+}$, n = 55, 110, and 140, were isolated, irradiated with electrons, and a variable delay after EC but prior to detection was added. For $Eu(H_2O)_{55}^{3+}$, an average water molecule loss due to EC of 17.04 and 17.11 occurs with a reaction delay of 40.4 ms and 1.00 s, respectively. The similar water loss indicates that dissociation of these clusters is rapid following EC and that any kinetic shift for clusters this size is negligible even for experiments as short as 40.4 ms. For $Eu(H_2O)_{110}^{3+}$, the average number of water molecules lost upon EC as a function of reaction delay time is shown in Figure 3. With a reaction delay of 40.4 ms after electron irradiation, the average number of water molecules lost upon EC is 16.1, whereas this value is 16.3 after 250 ms. This value remains essentially constant for longer reaction delays up to 1.50 s. These results indicate that dissociation is complete on a time scale between 40.4 and 250 ms for this cluster size. For $Eu(H_2O)_{140}^{3+}$, an average of 15.34 and 15.32 water molecules are lost from the reduced cluster with a reaction delay of 1.00 and 1.50 s, respectively. This indicates that a reaction delay of 1.00 s is sufficient to ensure that any effects of a kinetic shift are negligible for clusters with $n \leq 140$, and this value was chosen for experiments at all cluster sizes.

Recombination Energies. In many methods used to measure ionization energies, such as photoelectron spectroscopy, vertical

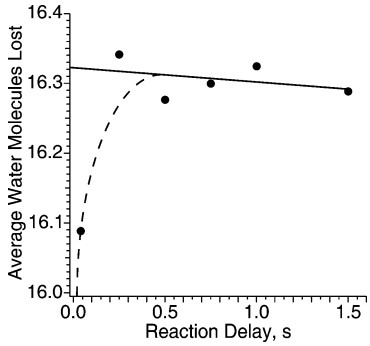

Figure 3. The average number of water molecules lost from $Eu(H_2O)_{110}^{3+}$ as a result of electron capture as a function of the reaction delay time between the end of electron capture and start of ion excitation and detection. The solid line is a linear regression best-fit line to the data from 0.250 to 1.50 s, and the dashed line is a guide for the eye.

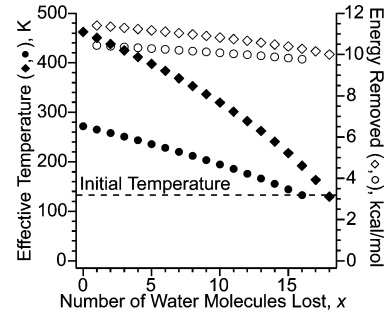

Figure 4. Modeled cluster effective temperatures (left axis, closed symbols) for $Eu(H_2O)_{n-x}^{2+}$ and the calculated sequential energy removed by the xth water molecule (right axis, open symbols) for $Eu(H_2O)_n^{3+}$, $n = 55$ (diamonds) and $n = 140$ (circles), activated by electron capture. The energy removed by each lost water molecule is obtained from the water molecule binding energy and the average energy partitioned into the translational and rotational modes of the products upon the loss of each water molecule. The dashed line indicates the temperature of the equilibrated ion cell and average temperature of the precursor ions prior to electron capture (133 K).

electron detachment energies are often obtained. In contrast, the recombination energy values obtained in these ion nanocalorimetry experiments correspond to adiabatic values because the time scale of water molecule reorganization (low picoseconds)[60−62] occurs much faster than the time scale of the experiment. In principle, RE values can be obtained from the sum of the sequential threshold dissociation (E_0) values for each water molecule lost from the reduced cluster that has lost the most water molecules. However, because some of the RE can partition into the translational, rotational, and vibrational modes of the water molecules that are lost, the probability that no energy partitions into these modes of any of the departing water molecules is infinitesimally small. Thus, in these nanocalorimetry experiments in which many water molecules are lost and where the signal-to-noise ratio is relatively low, the RE is obtained from the average number of water molecules lost, the sum of the sequential E_0 values, and from the energy partitioned into the translational, rotational, and vibrational modes of the products. Because the sequential binding energies to these large clusters have not been measured, the Thomson liquid drop model is used to calculate the binding energies of water molecules in these clusters.[63,64] Calculated binding enthalpies from a discrete implementation of this model reproduce experimental binding enthalpies within 1 kcal/mol for the largest cluster ions for which accurate experimental binding enthalpies have been reported.[64] These calculated values should be significantly more accurate for the larger clusters investigated here. At large n, the calculated water molecule binding enthalpies are comparable to the bulk heat of vaporization, consistent with the approach of the experimentally measured binding enthalpies to this value at relatively small cluster sizes ($n > 14$) even for clusters with divalent ions.[64]

To determine the energy released into the translational, rotational, and vibrational modes of the products upon the loss of water molecules, the cluster effective temperatures are modeled statistically[48] by solving for the cluster internal energies that give the observed average water molecule loss. For example, the calculated cluster effective temperatures for $Eu(H_2O)_{55-x}^{2+}$ and $Eu(H_2O)_{140-x}^{2+}$ are shown in Figure 4 (closed symbols). Upon EC, the reduced precursors heat to 460 and 270 K for the $n = 55$ (diamonds) and 140 (circles) clusters, respectively; the lower temperature of the $n = 140$ cluster is due to both a smaller RE value and a much larger number of degrees-of-freedom than the $n = 55$ cluster. Subsequent sequential water molecule loss cools the clusters to a temperature close to that of the ion cell (133 K, dashed line). From the cluster effective temperatures, T^*, the average energy lost to the translational and rotational modes of the ionic and neutral products, $(5/2)kT^*$, where k is the Boltzmann constant,[65−68] is obtained for each water molecule evaporated. Under these conditions, vibrational excitation of the lost water molecules should be negligible. The energy removed by each water molecule, that is, the sum of the binding energy and the energy partitioned into the translational, rotational, and vibrational modes, is shown in Figure 4 (open symbols) for the $Eu(H_2O)_{55-x}^{3+}$ (diamonds) and $Eu(H_2O)_{140-x}^{3+}$ (circles) precursor clusters. For example, the first water molecule lost from reduced $Eu(H_2O)_{55}^{3+}$ removes 11.5 kcal/mol, and the last water molecule lost removes 10.1 kcal/mol of energy. For reduced $Eu(H_2O)_{140}^{3+}$, the first and last water molecules lost remove 10.5 and 9.8 kcal/mol of energy, respectively. The sequential energy loss is greater for $Eu(H_2O)_{55}^{3+}$ than for $Eu(H_2O)_{140}^{3+}$ (◇ vs ○) predominantly because of the higher cluster effective temperatures for the smaller cluster resulting in more energy partitioned into translational and rotational modes of the products, although there are slight binding energy differences (≤0.2 kcal/mol) due to the substantially different cluster sizes.

To determine the effects of precursor cluster temperature on the RE values obtained via this method, measurements were performed on $Eu(H_2O)_{110}^{3+}$ at ion cell temperatures between −90 and −140 °C. An average number of 15.5, 15.6, and 15.8 water molecules were lost as a result of EC for ion cell temperatures of −90, −110, and −140 °C, respectively; these correspond to respective RE values of 7.01, 6.99, and 7.02 eV. These RE values are essentially the same despite the different

(60) Fecko, C. J.; Eaves, J. D.; Loparo, J. J.; Tokmakoff, A.; Geissler, P. L. *Science* **2003**, *301*, 1698–1702.
(61) Fecko, C. J.; Loparo, J. J.; Roberts, S. T.; Tokmakoff, A. *J. Chem. Phys.* **2005**, *122*, 1–18.
(62) Ohmine, I.; Tanaka, H. *Chem. Rev.* **1993**, *93*, 2545–2566.
(63) Holland, P. M.; Castleman, A. W., Jr. *J. Phys. Chem.* **1982**, *86*, 4181–4188.
(64) Donald, W. A.; Williams, E. R. *J. Phys. Chem. A* **2008**, *112*, 3515–3522.
(65) Klots, C. E. *J. Chem. Phys.* **1985**, *83*, 5854–5860.
(66) Klots, C. E. *J. Chem. Phys.* **1976**, *64*, 4269–4275.
(67) Klots, C. E. *J. Chem. Phys.* **1973**, *58*, 5364–5367.
(68) Klots, C. E. *Z. Naturforsch., A: Phys. Sci.* **1972**, *27A*, 553–561.

Scheme 1

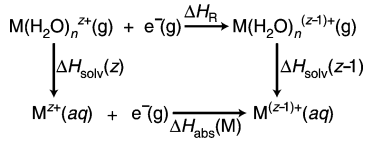

number of water molecules lost because more energy is partitioned into the translational and rotational modes of the products at higher cell temperatures due to the greater cluster internal energies at these temperatures. These results indicate that the RE values are not sensitive to initial cluster temperatures over this temperature range.[69]

Extrapolation of Absolute ΔH_R Values of $Eu(H_2O)_n^{3+}$ to the Condensed Phase. The gas-phase reduction enthalpy of a metal ion containing cluster is related to the solution-phase reduction enthalpy of the metal ion by the difference in the solvation enthalpies of the precursor and reduced precursor (Scheme 1), where the ΔH_R is the enthalpy of recombination ($\Delta H_R = -RE - c_{el}$, where c_{el} is the integrated heat capacity of the electron from Fermi−Dirac statistics),[70] $\Delta H_{solv}(z)$ and $\Delta H_{solv}(z-1)$ are the solvation enthalpies of the respective $z+$ and $(z-1)+$ clusters, and $\Delta H_{abs}(M)$ is the absolute solution-phase reduction enthalpy of $M^{z+}(aq)$. The absolute reduction Gibbs free energy of $M^{z+}(aq)$ can be obtained by combining the $\Delta H_{abs}(M)$ value with the absolute entropy term ($T\Delta S$) from solution-phase measurements. From the solution-phase absolute reduction free energy, the absolute potential of the redox active species in solution is obtained from the Faraday relation ($\Delta G = -nFE°$).

One approach to obtain bulk reduction potentials of metal ions in solution that does not require any ion solvation models like our previous methods[48,50] is to extrapolate absolute RE measurements to infinite cluster size to determine the energy of the corresponding process in the condensed phase. From the Scheme 1 thermodynamic cycle,

$$\Delta H_R = \Delta H_{abs}(M) + \Delta\Delta H_{solv} \quad (3)$$

where $\Delta\Delta H_{solv}$ is the difference between the solvation enthalpies of the $z+$ and $(z-1)+$ cluster ions. The solvation enthalpy of a cluster ion is proportional to the inverse of the cluster radius (R) for sufficiently large cluster ions that can be approximated by a sphere. The volume of a sphere is proportional to n, so that the radii of the clusters should be proportional to $n^{1/3}$, and $1/R$ is proportional to $n^{-1/3}$. Thus, eq 3 can be rewritten as

$$\Delta H_R(n) = \Delta H_{abs}(M) + Cn^{-1/3} \quad (4)$$

where C is a constant and $\Delta H_R(n)$ is the measured reduction enthalpy as a function of n. Thus, for sufficiently large clusters that can be approximated by a sphere, a plot of the measured $\Delta H_R(n)$ values versus $n^{-1/3}$ should result in a line with a y-axis intercept corresponding to $\Delta H_{abs}(M)$. This functional dependence is the same as that used to obtain the photoelectric threshold of bulk water by extrapolating vertical electron binding energies of gas-phase hydrated electron clusters to infinite cluster size.[37,38]

(69) At temperatures above −90 °C, the cluster ion abundance was too low to perform EC measurements. At temperatures below −140 °C, the instrument pumping efficiency dramatically decreased, and the ion signal became unstable.
(70) Bartmess, J. E. *J. Phys. Chem.* **1994**, *98*, 6420–6424.

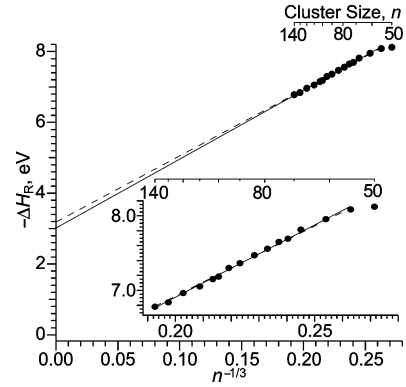

Figure 5. The negative of the measured $Eu(H_2O)_n^{3+}$ cluster recombination enthalpies vs $n^{-1/3}$. The solid line is a linear regression best-fit line, and the dashed line is a best-fit line using a slope (18.76 eV) calculated using the Born solvation model. The y-axis intercept of the former line corresponds to the absolute solution-phase reduction enthalpy of the $Eu^{3+/2+}$ half-cell (-3.03 ± 0.06 eV). The precursor cluster sizes, n, for each measurement are indicated on the top horizontal axis.

The negative of the recombination enthalpies of $Eu(H_2O)_n^{3+}$ as a function of $n^{-1/3}$ is shown in Figure 5. These data are linear from $n = 55$ to 140, from which a regression analysis results in a line with a y-axis intercept of 3.03 eV and a precision ±0.06 eV (Figure 5, solid line). The slope and R^2 values are 19.38 and 0.997, respectively. The linear dependence of the recombination enthalpies as a function of $n^{-1/3}$ at larger sizes ($n \geq 55$) indicates that ion solvation accounts for the vast majority of the decrease in the recombination enthalpies with increasing cluster sizes and that the y-axis intercept of the linear regression best-fit line (-3.03 ± 0.06 eV) corresponds to the absolute $Eu^{3+/2+}$ reduction enthalpy in aqueous solution. This extrapolation extends over a range of nanodrop diameters from about 1.5 to 2.0 nm. The slightly lower recombination enthalpy value for the $n = 50$ cluster than that predicted by the fitted line for the larger clusters suggests that other effects in addition to ion solvation have a slight role in cluster sizes smaller than ~55 water molecules. The absolute reduction potential of the $Eu^{3+/2+}$ redox reaction can be obtained from solution-phase experimental measurements of the absolute entropy[71,72] and our measured absolute solution-phase reduction enthalpy. This results in a value of −3.75 eV (+3.75 V) for the absolute solution-phase reduction free energy of Eu^{3+}. Combining the absolute reduction potential of $Eu^{3+/2+}$ from our nanocalorimetry method with the relative reduction potential of $Eu^{3+/2+}$ versus the SHE (−0.36 V),[73] a value of +4.11 V for the absolute SHE potential is obtained.

It is interesting to compare the linear regression best-fit line to the best-fit line obtained using a slope of 18.76 eV that is calculated using a modified Born solvation enthalpy calculation (Figure 5, dashed line).[74,75] The vertical deviation from the best-fit line is ±0.026 eV versus ±0.028 eV for the line obtained from Born solvation theory, indicating that both lines fit the data very well. From the y-axis intercept of latter line (3.17 eV), an absolute SHE value of +4.24 V is obtained. This value

(71) Bratsch, S. G. *J. Phys. Chem. Ref. Data* **1989**, *18*, 1–21.
(72) de Bethune, A. J.; Licht, T. S.; Swendeman, N. *J. Electrochem. Soc.* **1959**, *106*, 616–625.
(73) Milazzo, G.; Caroli, S.; Sharma, V. K. *Tables of Standard Electrode Potentials*; Wiley: Chichester, 1978.
(74) Born, M. *Z. Physik.* **1920**, *1*, 45–48.
(75) This slope was calculated using an effective water molecule radius of 1.93 Å and dielectric constant of 78.5.

is obtained essentially in the same way as in the single-cluster direct-reduction method[48] except that this value is an average of many measurements for different size clusters containing the same metal ion. The differences in the slope of the best-fit line (19.38 eV) as compared to that predicted by the Born solvation model (18.76 eV) may be due to uncertainties inherent in a continuum solvation model that does not explicitly account for quantum mechanical interactions between the solvating medium and the solvated ion and uncertainties in the parameters used to calculate the solvation enthalpy, such as the radii of the precursor and reduced precursor clusters, the dielectric constant of the solvent (ε), and $\partial \ln \varepsilon/\partial T$. The effects that these parameters have on the calculated cluster ion solvation enthalpies have been discussed previously.[48]

Sources of Uncertainty. Although the accuracy of this extrapolation method is difficult to assess, the precision is excellent ($\pm$0.06 eV). The greatest uncertainty is likely in the values used for the energy removed by evaporation of each water molecule from the reduced cluster. Both the water binding energies and the energy partitioned into translational and rotational modes of the products are obtained from well-established models, and uncertainties in these values are difficult to evaluate because of the lack of any experimental data for clusters this size. Photodissociation experiments done on large hydrated clusters of different charge states and size could be used to calibrate these models and would greatly reduce the uncertainty. For example, photodissociation of $Eu(H_2O)_{68}^{2+}$ using 157 nm light from a F_2 excimer laser would deposit 7.9 eV into this cluster, an energy equal to that calculated from the average water molecules lost upon EC by $Eu(H_2O)_{61}^{3+}$. Any difference would indicate an error in the modeled values. Similarly, light at different frequencies could be used to bracket our experimental data. Because the energy deposited in laser photodissociation can be very narrow, laser photodissociation data can be used to accurately calibrate the nanocalorimetry method so that no modeling of the experimental EC data would be required to obtain recombination energies.

Another source of uncertainty is that a long extrapolation to infinite cluster size (data for $n^{-1/3}$ between 0.1926 and 0.2630 extrapolated to zero) is required due to the range of cluster sizes that can be investigated with the current experimental apparatus. Similar long extrapolations are routinely used in Arrhenius analysis where kinetic data measured over a limited temperature range are extrapolated to infinite temperature to obtain accurate entropies of chemical reactions.[76,77] Data measured over a limited temperature range where measurements are possible are also extrapolated to zero temperature in equilibrium experiments to determine reaction enthalpies.[30,78] Despite the long extrapolations used in these methods, highly accurate thermochemical information can be obtained because of the high precision possible in these measurements. The precision of our extrapolation method is excellent ($\pm$0.06 eV), which can be attributed to the reproducibility with which these data can be obtained and to the large number of cluster measurements over a reasonably wide range of sizes. The uncertainty in the average number of water molecules, propagated from the signal-to-noise ratios for the relevant ion abundances in each mass spectrum, ranges from 0.04 to 0.13 water molecules for $Eu(H_2O)_n^{3+}$, n = 50−140, and the average of all of these values is 0.07 water molecules ($\sim$0.7 kcal/mol). The linearity of the Figure 5 data indicates that the structure of water in these nanodrops does not change significantly over this size range, consistent with limited data obtained from infrared photodissociation spectroscopy (vide infra) that indicate structures similar to that of bulk water. The accuracy of the absolute potential could be further improved by making these measurements on even larger clusters. The size clusters that can be investigated are limited by the magnetic field strength of our current apparatus. Because many performance characteristics of FT/ICR mass spectrometry, including ion storage capabilities and m/z range, scale with the square of the magnetic field strength,[79] measurements on clusters with over 900 water molecules could be made at 7.0 T ($7.00^2/2.75^2 \times 140 = 907$).

There are other possible sources of systematic error, including the estimation of the cluster volume, which depends on the effective size of the metal ion and its effect on the effective volume of the surrounding water molecules. We estimate the uncertainty arising from the effect of the ion on the cluster volume by including the average of the effective ionic volumes of Eu^{3+} and Eu^{2+}, $\bar{a}_i = 0.23$,[80−82] which corresponds to increasing the volume of the cluster by 0.23 water molecules; by using $(n + \bar{a}_i)$ in our analysis with $\bar{a}_i = +0.23$, a value for the absolute SHE potential of +4.10 V is obtained. It is also possible that the multivalent metal ion reduces the volume of the cluster versus that of bulk water due to the strong electrostatic interactions with the inner shell water molecules; a value of $\bar{a}_i = -0.23$ results in an absolute SHE potential of +4.12 V. Because of the difficulty of assessing the effect of the ion on cluster volume and because the effect of the physical size of the ion is likely to be counteracted by the ion−water attraction for inner shell water molecules, a value of $\bar{a}_i = 0$ appears to be reasonable and unlikely to be a significant source of error.

Another factor is radiative cooling of the cluster following EC, the rate of which depends on cluster size and could potentially result in a lower number of water molecules lost with increasing cluster size, and consequently a lower absolute SHE value. This effect for the smaller clusters should be negligible because water evaporation occurs in <40 ms, a time scale in which radiative emission should not be competitive. EC dissociation rates decrease with increasing cluster sizes so that radiative cooling could be more competitive, but the effective temperatures of these clusters are also lower due to more degrees-of-freedom and lower REs, which reduce radiative cooling rates. The absence of any curvature in the Figure 5 data suggests that effects of radiative cooling are negligible over this cluster size range. Modeling of radiation processes for these clusters is currently underway.

Another potential size-dependent effect could arise from the BIRD correction, in which the average number of water molecules lost due to EC alone is estimated from the average

(76) Benson, S. W.; O'Neal, H. E. *Kinetic Data on Gas Phase Unimolecular Reactions*; U.S. National Bureau of Standards: Washington, 1970.
(77) Schnier, P. D.; Price, W. D.; Jockusch, R. A.; Williams, E. R. *J. Am. Chem. Soc.* **1996**, *118*, 7178–7189.
(78) Gao, B.; Wyttenbach, T.; Bowers, M. T. *J. Am. Chem. Soc.* **2009**, *131*, 4695–4701.
(79) Marshall, A. G.; Guan, S. *Rapid Commun. Mass Spectrom.* **1996**, *10*, 1819–1823.
(80) The value of $\bar{a}_i$ is calculated using the effective radii of trivalent (1.275 Å) and divalent (1.093 Å) europium ions and that of a bulk water molecule, from the density of bulk water at 298 K (0.9970 g/cm^3) from refs 81 and 82.
(81) Shannon, R. D. *Acta Crystallogr.* **1976**, *A32*, 751–767.
(82) Marsh, K. N. *Recommended Reference Materials for the Realization of Physiochemical Properties*; Blackwell: Oxford, 1987.

number of water molecules lost from the reduced precursor corrected for the average loss from the precursor. This approximation should become better with increasing cluster sizes because the sizes of the precursor and reduced precursor become more comparable. The average number of water molecules lost due to EC alone is essentially constant over a wide range of reaction delays for the $n = 110$ cluster (250 ms to 1.50 s) and $n = 55$ cluster (40.4 ms to 1.00 s), which strongly indicates that this effect is negligible.

There is also uncertainty in the solution-phase relative reduction potential of the $Eu^{3+/2+}$ half-cell potential. In noncomplexing supporting media, standard potential values of between −0.35 and −0.38 V for the one-electron reduction of aqueous Eu^{3+} versus the SHE have been reported.[83−91] An average of six independent measurements from six different groups[83−88] results in a potential of -0.36 ± 0.02 V, consistent with the tabulated value reported by Milazzo et al.[73] This agrees with other tabular sources[71,92,93] that reference a value of -0.35 ± 0.03 V, which is based on an average of three independent measurements[86,87,90] that do not include what appear to be the two most recent measurements.[83,88] Here, we use a value of −0.36 V for the $Eu^{3+/2+}$ half-cell potential. The absolute entropy term ($T\Delta S$) of the SHE half-cell reaction (0.260 eV)[72] used in this method agrees with another reported value of 0.262 ± 0.002 eV[94] and should not be a significant source of error. The latter experiment investigated and accounted for salt-bridge effects on the value obtained.[94]

Ion Coordination and the Nanodrop Surface Structure. Two important questions must be addressed to extrapolate bulk physical properties from these nanodrop experiments. First, is the ion coordination in the nanodrops the same as that in bulk solution? Second, because the absolute SHE potential includes a contribution for the surface potential of the bulk air−water interface due to the orientation of water molecules at this interface, is the surface potential of these nanodrops the same as that of the bulk air−water interface? We address both of these questions below.

Ion coordination numbers (CNs) can be obtained from gas-phase measurements of small clusters using a variety of different methods. However, relating these values to those in bulk solution can be complicated by many factors. For example, a CN of 6 for Ca^{2+} has been deduced in small gaseous water clusters from high pressure mass spectrometry,[95] blackbody infrared radiative dissociation,[96,97] guided ion beam mass spectrometry,[98] infrared photodissociation (IRPD) spectroscopy experiments,[99] and theory,[97,98,100] although some support for a CN = 7 has also been reported.[96,97] In solution, Ca^{2+} has been investigated using a variety of methods, including X-ray,[101−105] neutron diffraction,[106−108] and theory.[105,109−115] Most studies indicate a CN between 7 and 8, although the full range of reported values is between 5 and 10.[101−115] Recent IRPD studies of size-selected gaseous $Ca(H_2O)_n^{2+}$ indicate that the CN of Ca^{2+} in these clusters changes from six for clusters with fewer than 12 water molecules to eight for clusters with 12 or more water molecules.[99,116] A CN of eight is consistent with results from many solution-phase studies and suggests that the local environment of Ca^{2+} in the larger gaseous clusters is similar to that in bulk water.

Further support for the similar local environment of the metal ions in these nanodrops to that in bulk solution is obtained from the reactivity of size-selected $M(H_2O)_n^{3+}$, M = La, Ce, Pr, Nd, Sm, Eu, Gd, Tb, Dy, Ho, Er, Tm, Lu, and Y.[117] These clusters undergo a charge separation reaction to produce $H(H_2O)_x^+$ and $MOH(H_2O)_y^{2+}$ at cluster sizes between 17 and 21 water molecules. Turnover sizes, where the branching ratios for the charge separation reaction and the loss of a water molecule are equal, showed a strong correlation with solution hydrolysis in which data for M = La to Gd and M = Sm to Lu were well fit by two lines that both share M = Sm, Eu, and Gd. The intercept between these lines is consistent with a "gadolinium break" in which a change in some physical properties occurs for ions in the middle (around Gd) of the series.[118−120] The correlation

(83) Elzanowska, H.; Galus, Z.; Borkowska, Z. *J. Electroanal. Chem.* **1983**, *157*, 251–268.
(84) Timmer, B.; Sluyters-Rehbach, M.; Sluyters, J. H. *J. Electroanal. Chem.* **1967**, *14*, 181–191.
(85) Gierst, L.; Cornelissen, R. *Collect. Czech. Chem. Commun.* **1960**, *25*, 3004–3015.
(86) Anderson, L. B.; Macero, D. J. *J. Phys. Chem.* **1963**, *67*, 1942.
(87) Morss, L. R.; Haug, H. O. *J. Chem. Thermodyn.* **1973**, *5*, 513–524.
(88) Biedermann, G.; Silber, H. B. *Acta Chem. Scand.* **1973**, *27*, 3761–3768.
(89) Rard, J. A. *Chem. Rev.* **1985**, *85*, 555–582.
(90) Biedermann, G.; Terjosin, G. S. *Acta Chem. Scand.* **1969**, *23*, 1896–1902.
(91) Macero, D. J.; Anderson, L. B.; Malachesky, P. *J. Electroanal. Chem.* **1965**, *10*, 76–81.
(92) *Standard Potentials in Aqueous Solutions*; Marcel Dekker: New York, 1985.
(93) Morss, L. R. *Chem. Rev.* **1976**, *76*, 827–841.
(94) Conway, B. E.; Wilkinson, D. P. *Electrochim. Acta* **1993**, *38*, 997–1013.
(95) Peschke, M.; Blades, A. T.; Kebarle, P. *J. Phys. Chem. A* **1998**, *102*, 9978–9985.
(96) Rodriguez-Cruz, S. E.; Jockusch, R. A.; Williams, E. R. *J. Am. Chem. Soc.* **1998**, *120*, 5842–5843.
(97) Rodriguez-Cruz, S. E.; Jockusch, R. A.; Williams, E. R. *J. Am. Chem. Soc.* **1999**, *121*, 8898–8906.
(98) Carl, D. R.; Moision, R. M.; Armentrout, P. B. *Int. J. Mass Spectrom.* **2007**, *265*, 308–325.
(99) Bush, M. F.; Saykally, R. J.; Williams, E. R. *ChemPhysChem* **2007**, *8*, 2245–2253.
(100) Pavlov, M.; Siegbahn, P. E. M.; Sandström, M. *J. Phys. Chem. A* **1998**, *102*, 219–228.
(101) Megyes, T.; Grosz, T.; Radnai, T.; Bako, I.; Palinkas, G. *J. Phys. Chem. A* **2004**, *108*, 7261–7271.
(102) Fulton, J. L.; Heald, S. M.; Badyal, Y. S.; Simonson, J. M. *J. Phys. Chem. A* **2003**, *107*, 4688–4696.
(103) Yamaguchi, T.; Hayashi, S.; Ohtaki, H. *Inorg. Chem.* **1989**, *28*, 2434–2439.
(104) Licheri, G.; Piccaluga, G.; Pinna, G. *J. Chem. Phys.* **1976**, *64*, 2437–2441.
(105) Probst, M. M.; Radnai, T.; Heinzinger, K.; Bopp, P.; Rode, B. M. *J. Phys. Chem.* **1985**, *89*, 753–759.
(106) Cummings, S.; Enderby, J. E.; Howe, R. A. *J. Phys. C: Solid State Phys.* **1980**, *13*, 1–8.
(107) Hewish, N. A.; Neilson, G. W.; Enderby, J. E. *Nature* **1982**, *297*, 138–139.
(108) Badyal, Y. S.; Barnes, A. C.; Cuello, G. J.; Simonson, J. M. *J. Phys. Chem. A* **2004**, *108*, 11819–11827.
(109) Naor, M. M.; Van Nostrand, K.; Dellago, C. *Chem. Phys. Lett.* **2003**, *369*, 159–164.
(110) Bounds, D. G. *Mol. Phys.* **1985**, *54*, 1335–1355.
(111) Pálinkás, G.; Heinzinger, K. *Chem. Phys. Lett.* **1986**, *126*, 251–254.
(112) Obst, S.; Bradaczek, H. *J. Phys. Chem.* **1996**, *100*, 15677–15687.
(113) Kalko, S. G.; Sesé, G.; Padró, J. A. *J. Chem. Phys.* **1996**, *104*, 9578–9585.
(114) Schwenk, C. F.; Loeffler, H. H.; Rode, B. M. *J. Chem. Phys.* **2001**, *115*, 10808–10813.
(115) Tongraar, A.; Liedl, K. R.; Rode, B. M. *J. Phys. Chem. A* **1997**, *101*, 6299–6309.
(116) Bush, M. F.; Saykally, R. J.; Williams, E. R. *J. Am. Chem. Soc.* **2008**, *130*, 15482–15489.
(117) Bush, M. F.; Saykally, R. J.; Williams, E. R. *J. Am. Chem. Soc.* **2008**, *130*, 9122–9128.
(118) Spedding, F. H.; Pikal, M. J.; Ayers, B. O. *J. Phys. Chem.* **1966**, *70*, 2440–2449.
(119) Spedding, F. H.; Jones, K. C. *J. Phys. Chem.* **1966**, *70*, 2450–2455.
(120) Spedding, F. H.; Pikal, M. J. *J. Phys. Chem.* **1966**, *70*, 2430–2440.

between the charge separation reaction in the gas phase and hydrolysis in solution suggests that the local environment of these ions in both phases is similar.

Information about the surface structure of these nanodrops can be obtained from IRPD spectroscopy experiments.[99,116,117,121−123] For $Ca(H_2O)_n^{2+}$, n up to 69,[99,116] the free OH stretches of surface water molecules in larger clusters can be readily observed and assigned to water molecules that accept either one or two hydrogen bonds and donate either one or no hydrogen bonds, based on the frequency of the free OH stretches. Results from the IRPD spectroscopy experiments indicate that the number of single acceptor water molecules at the cluster surface is essentially zero by $n \approx 30$, and the spectra of the largest clusters have only subtle changes with increasing cluster size. These spectra indicate that the majority of the surface water molecules with a free OH stretch in the larger clusters accept two hydrogen bonds and donate a single hydrogen bond, consistent with what is known about the structure of water at the bulk air−water interface.[124−128] Recent IRPD spectroscopy results on $La(H_2O)_n^{3+}$ with n up to 161 indicate that the frequency of the free OH stretch of the double-acceptor single-donor surface water molecules does not change with cluster size above $n = \sim 100$ and is about the same as that measured at the air−water interface in sum frequency generation experiments.[124−128] These results suggest that the orientations of surface water molecules do not change significantly for clusters in this size range and that the surface water molecules in these nanodrops are similar to those at the bulk air−water interface. The spectra of the bonded OH region for these clusters appear similar to the infrared spectrum of bulk water in this region,[129] suggesting that the interior water molecules in these clusters also resemble those in bulk solution.

An ensemble averaged IRPD spectrum of $Eu(H_2O)_n^{3+}$, with $n = 119-124$, which is indistinguishable from IRPD spectra of comparable-size nanodrops containing La^{3+}, is shown in Figure 6. The sharp feature at 3694 cm^{-1} corresponds to the free OH stretch of surface water molecules that accept two hydrogen bonds and donate one hydrogen bond, and the band occurs at nearly the same frequency as that for surface water molecules in sum frequency generation spectra of the bulk air−water interface (~3700 cm^{-1}).[124−128] The less intense sharp band at 3716 cm^{-1} corresponds to surface water molecules that accept and donate a single hydrogen bond. The broad peak centered at ~3430 cm^{-1} corresponds to hydrogen-bonded OH stretches. The frequency and width of this band are similar to that in the transmittance FTIR spectrum of liquid water in this region.[129] A more detailed discussion of the IRPD spectra and structures of size-selected $La(H_2O)_n^{3+}$ will be presented elsewhere.

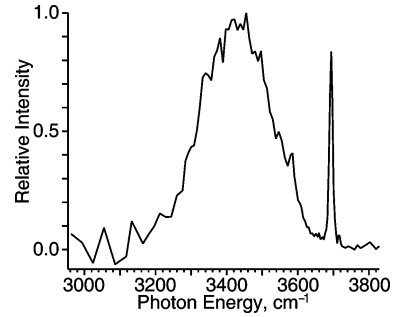

Figure 6. Ensemble infrared photodissociation spectrum of $Eu(H_2O)_n^{3+}$, $n = 119-124$, at 133 K. The photodissociation intensity is obtained from the average number of water molecules lost due to absorption of infrared radiation from a wavelength tunable OPO/OPA laser system corrected for absorption of blackbody infrared photons and laser power.

The results from these IRPD experiments indicate that both the ion coordination number and the hydrogen-bonding environment of surface water molecules on the nanodrops should be very close to those in bulk solution. Although the surface potential of bulk water is not accurately known and has not been directly measured,[19] many estimates[4,15,19,130] and quantum chemical ab initio theoretical results[18] indicate that this potential is relatively small. Thus, any differences in the surface of these nanodrops from that in bulk solution should contribute negligibly to any uncertainties in these absolute reduction enthalpy measurements. The linearity of the RE values for $Eu(H_2O)_n^{3+}$ as a function of $n^{-1/3}$ also indicates that the surface potential of these nanodrops does not change significantly over this size range or that this effect is small.

Real Solvation Energy of the Proton from Gaseous Cluster Measurements. If the absolute potential of the SHE is known, the real proton solvation energy can be obtained from eq 1. The absolute SHE potential value obtained from this extrapolation method (+4.11 V) corresponds to a value of −269.0 kcal/mol for the real proton solvation energy. This value of $\alpha(H^+,aq)$ is more negative than that reported by Farrell and McTigue (−260.0 kcal/mol[15] revised to −261.3 kcal/mol using Fermi−Dirac statistics for the heat capacity of the electron and to have the same gas and solution-phase concentration[50]) and by Fawcett (−260.7 kcal/mol).[8] However, our value agrees reasonably well with that obtained using the cluster-pair correlation method (−265.9 kcal/mol; using the same reference state as Truhlar and co-workers)[6,7,24] and that obtained computationally by Goddard and co-workers (−266.7 kcal/mol).[21] These latter values may not accurately account for the surface potential because of the small cluster sizes used.[8] However, if the surface potential of water is small, as indicated by recent ab initio molecular dynamics calculations,[18] then our experimentally measured value is in reasonable agreement with values obtained from these two recent studies.

Conclusions

We have demonstrated three largely independent methods that use ion nanocalorimetry to obtain a value for the absolute SHE potential that ranges from +4.05 to +4.21 V.[48,50] In our previous two nanocalorimetry methods, the cluster solvation enthalpies are calculated from the Born solvation model, which is a continuum model that does not explicitly account for quantum mechanical interactions between the ion and solvent. A key

(121) Shin, J.-W.; Hammer, N. I.; Diken, E. G.; Johnson, M. A.; Walters, R. S.; Jaeger, T. D.; Duncan, M. A.; Christie, R. A.; Jordan, K. D. *Science* **2004**, *304*, 1137–1140.
(122) Miyazaki, M.; Fujii, A.; Ebata, T.; Mikami, N. *Science* **2004**, *304*, 1134–1137.
(123) Walters, R. S.; Pillai, E. D.; Duncan, M. A. *J. Am. Chem. Soc.* **2005**, *127*, 16599–16610.
(124) Gopalakrishnan, S.; Liu, D.; Allen, H. C. *Chem. Rev.* **2006**, *106*, 1155–1175.
(125) Shultz, M. J.; Schnitzer, C.; Simonelli, D.; Baldelli, S. *Int. Rev. Phys. Chem.* **2000**, *19*, 123–153.
(126) Shen, Y. R.; Ostroverkhov, V. *Chem. Rev.* **2006**, *106*, 1140–1154.
(127) Richmond, G. L. *Chem. Rev.* **2002**, *102*, 2693–2724.
(128) Ji, N.; Ostroverkhov, V.; Tian, C. S.; Shen, Y. R. *Phys. Rev. Lett.* **2008**, *100*, 096102.
(129) Freda, M.; Piluso, A.; Santucci, A.; Sassi, P. *Appl. Spectrosc.* **2005**, *59*, 1155–1159.
(130) Borazio, A.; Farrell, J. R.; McTigue, P. *J. Electroanal. Chem.* **1985**, *193*, 103–112.

advantage of the extrapolation method demonstrated here is that a solvation model is not required, which eliminates the accompanying uncertainties associated with models, making this the most direct method to obtain the absolute SHE potential. For these reasons, the value of +4.11 V obtained by this method is likely more accurate than those obtained from our other two ion nanocalorimetry methods.

A more accurate value for the absolute SHE potential could be obtained using our extrapolation method by (1) calibrating the recombination energy values using laser photodissociation experiments at multiple wavelengths, cluster sizes, and charge states, (2) increasing the magnetic field strength of the experimental apparatus from 2.7 to 7.0 T, which would increase the size of the clusters that could be studied to ~900 water molecules, and (3) measuring other redox couples. By combining this extrapolation method with laser calibrated nanocalorimetry data, an absolute reduction potential could be directly measured with no modeling necessary. This would be the most direct route to experimentally measuring an absolute reduction potential. Combined with the other proposed improvements, an absolute reduction potential could be directly measured for a single redox couple with accuracy better than ±0.05 V, which could then be used to establish an absolute electrochemical scale.

The absolute reduction potential obtained in our nanocalorimetry experiments does not include effects from counterions or supporting electrolytes, junction potentials, or other effects from liquid/metal or metal/metal interfaces because such effects are absent in our measurements. This method has the advantage that counterion effects on reduction potentials can be investigated by careful control of the nanodrop content. This method could also be used to investigate reduction energies of ions in solvents in which electrochemistry is difficult or impossible to perform with conventional methods. These ion nanocalorimetry experiments illustrate that gas-phase ionization/reduction energies and solution-phase redox potentials can be directly related from size-selected cluster measurements and that these measurements can provide new insights into effects of ion solvation.

Acknowledgment. We thank the National Institutes of Health (Grant R01GM064712-08), the National Science Foundation (CHE-0718790), and the ACS Petroleum Research Fund (47916-AC6) for generous financial support, and the Eastman Chemical Co. for sponsoring an ACS Division of Analytical Chemistry Summer Fellowship for W.A.D.

Supporting Information Available: Revision of absolute SHE potential reported in reference 50. This material is available free of charge via the Internet at http://pubs.acs.org.

JA902815V